

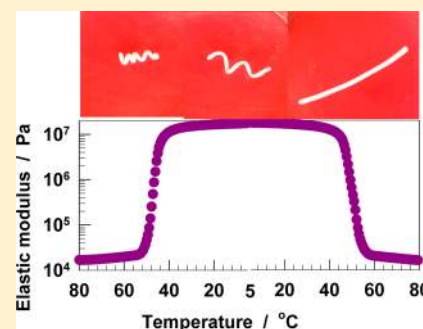
# Shape Memory Hydrogels via Micellar Copolymerization of Acrylic Acid and *n*-Octadecyl Acrylate in Aqueous Media

Cigdem Bilici and Oguz Okay\*

Department of Chemistry, Istanbul Technical University, 34469 Maslak, Istanbul, Turkey

**S** Supporting Information

**ABSTRACT:** A novel way for the production of shape memory hydrogels containing crystalline domains is described. Hydrogels were prepared by micellar copolymerization of acrylic acid with the hydrophobic comonomer *n*-octadecyl acrylate (C18) in an aqueous NaCl solution of sodium dodecyl sulfate (SDS). The presence of NaCl causes the SDS micelles to grow and thus enables solubilization of large amounts (16% w/v) of C18 in the micellar solution. DSC measurements show that the swollen hydrogels, possessing 61–84% water, melt and crystallize with a change in temperature. Independent of the hydrophobe level between 20 and 50 mol %, the melting and crystallization temperatures of the hydrogels are  $48 \pm 2$  and  $43 \pm 2$  °C, respectively. The hydrogels exhibit 3 orders of magnitude change in the elastic modulus when the temperature changes between below and above the melting temperature of the crystalline domains. The blocky structure of the network chains formed by micellar polymerization is responsible for the drastic change in their mechanical properties and significant shape memory effect.



## INTRODUCTION

Aqueous solutions of hydrophobically modified hydrophilic polymers constitute a class of soft materials with remarkable rheological properties.<sup>1,2</sup> A simple method to obtain such associative polymers is the free radical micellar polymerization technique, as first described by Candau and co-workers.<sup>1–8</sup> In this technique, a water-insoluble hydrophobic monomer solubilized within the micelles is copolymerized with a hydrophilic monomer such as acrylamide (AAm) or acrylic acid (AAc) in aqueous solutions by free-radical addition polymerization. Because of high local concentration of the hydrophobe within the micelles, the hydrophobic monomers are distributed as random blocks along the hydrophilic polymer backbone. One limitation of this technique is that large hydrophobes cannot be solubilized within the micelles due to the very low water solubility of these monomers.<sup>9–11</sup> We have recently shown that *n*-alkyl (meth)acrylates with an alkyl chain length longer than 16 carbon atoms can be solubilized in a micellar solution of sodium dodecyl sulfate (SDS) provided that an electrolyte, such as NaCl, has been added in sufficient amount.<sup>12</sup> Salt leads to micellar growth and, hence, solubilization of the hydrophobes within the grown SDS micelles. Copolymerization of AAm with large hydrophobes solubilized within the wormlike SDS micelles produced physical hydrogels exhibiting unique characteristics such as insolubility in water, non-ergodicity, high elongation ratios at break, and self-healing.<sup>12–15</sup>

Hydrophobe content of the physical gels having the ability to self-heal was 2 mol % with respect to the total monomers while the self-healing ability disappeared as the hydrophobe content is increased.

Here, we report that the micellar polymerization at a high hydrophobe level (20–50 mol %) leads to the formation of hydrogels containing crystalline domains and exhibiting shape memory properties. Hydrogels were prepared by copolymerization of AAc and *n*-octadecyl acrylate (C18) in aqueous SDS–NaCl solutions. To stabilize the permanent shape of the hydrogels, *N,N'*-methylenebis(acrylamide) as a chemical cross-linker was also included in the monomer mixture. These hydrogels possess 61–84% water and exhibit 3 orders of magnitude change in the elastic modulus when the temperature changes between below and above the melting temperature of the crystalline domains. The hydrogels exhibit complete shape recovery to the permanent shape within 20 s at 60 °C. To our knowledge, the micellar polymerization technique has not been reported before for the preparation of hydrogels with shape memory effect. However, several studies report preparation of shape memory hydrogels by hydrophobic associations.<sup>16–24</sup> Osada was the first to prepare such hydrogels by solution copolymerization of AAc and C18 in an organic media.<sup>16–19</sup> It was shown that the gels exhibit up to 120-fold modulus change with a change in temperature due to the presence of crystalline domains. Since the blocky structure of hydrophobically modified polymers formed by micellar polymerization enhances significantly their associative properties, present hydrogels exhibit 1000-fold change in their elastic moduli in response to temperature and thus stronger shape memory effect. The synthesis strategy presented here could be extended to different

Received: March 8, 2013

Revised: April 3, 2013

Published: April 12, 2013

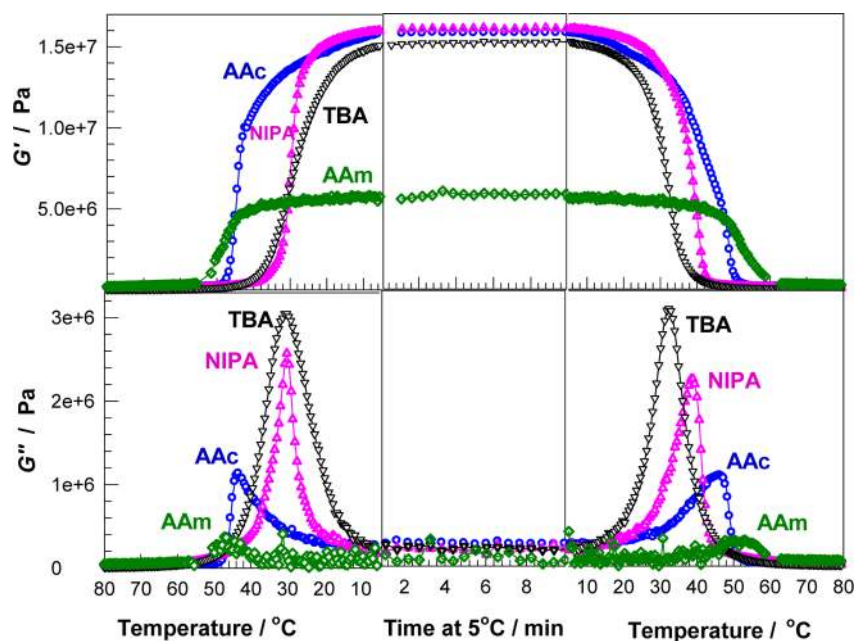


**Figure 1.** Viscoelastic behavior of equilibrium swollen hydrogels during the cooling–heating cycle between 80 and 5 °C. The hydrogels were prepared by random copolymerization of C18 with the hydrophilic monomers indicated. C18 = 35 mol %,  $X = 1/100$ ,  $\omega = 6.28$  rad/s, and  $\gamma_0 = 0.001$ .

hydrophilic and hydrophobic monomers as well as surfactant–salt systems to generate shape memory hydrogels with tunable properties.

## EXPERIMENTAL PART

**Materials.** *n*-Octadecyl acrylate (C18, Aldrich), *N,N'*-methylenebis(acrylamide) (BAAm, Merck), *N*-isopropylacrylamide (NIPA, Aldrich), *N-tert*-butylacrylamide (TBA, Fluka), acrylamide (AAm, Merck), sodium dodecyl sulfate (SDS, Sigma), NaCl (Merck), ammonium persulfate (APS, Sigma), sodium metabisulfite (SMS, Merck), 2,2'-azobis(isobutyronitrile) (AIBN, Fluka), and ethanol (Merck) were used as received. Acrylic acid (AAc, Merck) was freed from its inhibitor by passing through an inhibitor removal column purchased from the Aldrich Chemical Co. APS and SMS stock solutions were prepared by dissolving 0.180 g of APS and 0.190 g of SMS separately in 10 mL of water.

**Quantification of the Solubilization of C18 in SDS–NaCl Solutions.** The amount of C18 solubilized in the micelles was estimated by measuring the transmittance of SDS (22% w/v)–NaCl (0–1.5 M) solutions at 55 °C containing various amounts of C18 on a T80 UV–vis spectrophotometer. The transmittance at 500 nm was plotted as a function of the added amount of C18 in the SDS–NaCl solution, and the solubilization extent of C18 was determined by the curve break (Figure S1).

**Determination of the Size of the Micelles.** The measurements on SDS–NaCl solutions were performed at 55 °C in the instrument Zetasizer Nano S from Malvern. The instrument contains a 4 mW He–Ne laser operating at a wavelength  $\lambda$  of 633 nm with a fixed detector angle of 173° and incorporates noninvasive backscatter optics. The data were analyzed by the cumulant method using Malvern application software, and the hydrodynamic correlation lengths  $\xi_{\text{H}}$  were obtained from the first cumulant.

**Hydrogel Preparation.** To determine the best hydrophilic comonomer of C18 for the synthesis of hydrogels containing crystalline domains, preliminary experiments were carried out using the hydrophilic monomers AAc, AAm, NIPA, and TBA. These experiments were carried out by random copolymerization of the hydrophilic monomer with C18 hydrophobe (35 mol % in the feed) in the presence of BAAm at a fixed cross-linker ratio  $X$  (moles of BAAm per mole of the monomers) of 0.01. The reactions were conducted at an initial monomer concentration of 3 M in the presence of AIBN initiator (0.03

M) in ethanol at 50 °C, as described previously.<sup>16</sup> Hydrogels with a gel fraction of unity could be obtained after a reaction time of 24 h. It was found that the chemical structure of the polymer backbone influences significantly the crystallization behavior of the hydrogels. The melting temperature of water-swollen hydrogels increased in the order TBA < NIPA < AAm = AAc (Figure S2). Thus, as compared to AAc or AAm, NIPA and TBA with bulky side groups decrease the melting temperature of the hydrogels. In Figure 1, the variations of the elastic modulus  $G'$  and the viscous modulus  $G''$  of water-swollen hydrogels with AAc, AAm, NIPA, and TBA units in the polymer backbone are shown during the cooling–heating cycle between 80 and 5 °C. In hydrogels containing NIPA or TBA units, the large energy dissipation at the transition regions is due to the association–dissociation of these units with temperature. Moreover, as compared to the hydrogels formed using AAm as the hydrophilic monomer, those formed using AAc exhibit a drastic change in the elastic modulus, which is attributed to the cooperative hydrogen bonding between the carboxyl groups stabilizing the crystalline domains.<sup>21</sup> These results reveal that AAc is the best choice for the preparation of hydrophobically modified hydrogels with most stable crystalline domains. In the following, the results obtained using AAc monomer will be presented.

Micellar polymerization of AAc with C18 hydrophobe and BAAm cross-linker was conducted at 55 °C in the presence of an APS (0.79 mM)–SMS (1 mM) redox initiator system. A 22% w/v SDS solution prepared in 1.5 M NaCl was used as the micellar solution. The cross-linker ratio  $X$  was set to 0.01. Three sets of gelation experiments were carried out at 20, 35, and 50 mol % C18 (with respect to the monomers), while the total monomer concentration was set to 0.75 and 1.0 M. To illustrate the synthetic procedure, we give details for the preparation of hydrogels at an initial monomer concentration of 1.0 M with 50 mol % C18 in the feed: SDS (2.2 g) was dissolved in 8.5 mL of water containing 0.8766 g of NaCl at 55 °C to obtain a transparent solution. Then, C18 (1.622 g) was dissolved in this SDS–NaCl solution under stirring for 30 min at 55 °C. After addition and dissolving AAc (0.3603 g) and BAAm (0.0154 g) for 30 min, stock solutions of SMS (0.1 mL) and APS (0.1 mL) were added to obtain a final reaction volume of 10 mL. For the rheological experiments, a portion of this solution was transferred between two glass plates (5 × 5 cm) separated by a 0.5 mm Teflon spacer. The remaining part of the reaction solution was transferred into several plastic syringes of 4.8 mm internal diameters. The polymerization was conducted for one day at 55 °C.

**Gel Fractions and Swelling Measurements.** Hydrogel samples were immersed in a large excess of water at 24 °C for at least 1 month by replacing water every day to extract any soluble species. SDS concentration in the external solutions (before refreshing) rapidly dropped below the detection limit of the methylene blue method<sup>25</sup> (0.20 mg L<sup>-1</sup>) after about 10 days, indicating completeness of SDS extraction from gel samples. The equilibrium swollen gel samples were taken out of water and dried at 55 °C under vacuum to constant mass. The water content of the hydrogels was estimated as  $H_2O\% = 1 - m_{dry}/m$ , where  $m$  and  $m_{dry}$  are the swollen and dry masses of the gel sample, respectively. The gel fraction  $W_g$ , i.e., the conversion of monomers to the cross-linked polymer (mass of cross-linked polymer/initial mass of the monomer), was calculated from the masses of dry, extracted polymer network and from the comonomer feed.

**Rheological Experiments.** The gel samples in the form of sheets were subjected to the rheological measurements between the parallel plates of the rheometer (Gemini 150 Rheometer system, Bohlin Instruments) equipped with a Peltier device for temperature control. The upper plate (diameter 40 mm) was set at a distance of 500–700  $\mu$ m, depending on the swelling degree of the hydrogels. During all rheological measurements, a solvent trap was used to minimize the evaporation. Further, the outside of the upper plate was covered with a thin layer of low-viscosity silicone oil to prevent evaporation of solvent. A frequency of  $\omega = 6.28$  rad/s and a deformation amplitude  $\gamma_0 = 0.001$  (0.1%) were selected to ensure that the oscillatory deformation is within the linear regime. Thermal behavior of the gels was investigated by first keeping the samples at 80 °C for complete melting and then cooling down to 5 °C, after keeping for 10 min at 5 °C, and heating back to 80 °C. The cooling/heating steps were carried out at a fixed rate of 1 °C/min. The changes in the dynamic moduli of gels were monitored during the course of the cycle as a function of temperature.

**DSC Measurements.** DSC measurements were conducted on a PerkinElmer Diamond DSC under a nitrogen atmosphere. The gel samples sealed in aluminum pans were scanned between 5 and 80 °C with a heating and cooling rate of 5 °C/min.

**X-ray Diffraction.** X-ray diffraction patterns of swollen hydrogel samples were collected on a Rigaku Miniflex diffractometer using a high power Cu K $\alpha$  source ( $\lambda = 0.154$  18 nm) operating at 30 kV/15 mA. The XRD patterns were collected in the 1°–50°, 2 $\theta$  range with scan rates of 1 and 0.5°/min.

**Shape Memory Behavior.** The shape memory effect was examined by a bending test as follows:<sup>22,26</sup> A cylindrical hydrogel sample (diameter 4.8 mm, length about 6 cm) was folded at 60 °C and then cooled to keep the deformation. The deformed hydrogel sample was immersed in a water bath at 25 °C and then stepwise heated from 25 to 70 °C at 1–3 °C steps. At each temperature  $T$ , the final angle  $\theta_T$  was recorded after it has been steady. The measurements of  $\theta_T$  were conducted using an image analyzing system consisting of a microscope (XSZ single Zoom microscope), a CDD digital camera (TK 1381 EG), and a PC with the data analyzing system Image-Pro Plus. The shape recovery ratio  $R$  was calculated as  $R = \theta_T/180$ .

## RESULTS AND DISCUSSION

The key step of our approach was to create suitable conditions so that large amounts of C18 could be solubilized in micellar solutions. This was achieved by the addition of NaCl into aqueous semidilute SDS solutions. Figure 2A,B demonstrates the NaCl-induced solubilization of C18 in an aqueous 22% w/v SDS solution. The hydrodynamic correlation length  $\xi_H$  of the solution (A) and the solubility of C18 (B) are plotted against NaCl concentration. As the salt concentration is increased,  $\xi_H$  also increases, indicating that the micelles grow bigger. The growth of the micelles is due to the change of the micellar structure of SDS from sphere to rod and then to large cylindrical aggregates or flexible wormlike micelles by the addition of salts.<sup>27</sup>

Assuming a prolate ellipsoidal shape for SDS micelles in aqueous NaCl and equating the semiminor axis  $b$  with the radius of the minimum spherical micelle (2.5 nm),<sup>28,29</sup> one may

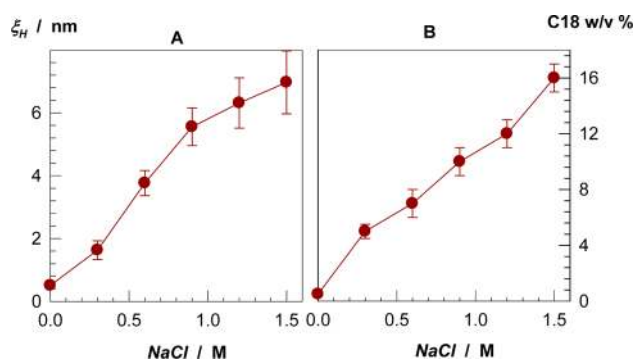


**Figure 2.** Hydrodynamic correlation length  $\xi_H$  of 22% w/v SDS solution (A) and the solubility of C18 (B) shown as a function of NaCl concentration. Temperature = 55 °C.

estimate the semimajor axis  $a$  of the micelles using Perrin's equations.<sup>30</sup> The radius  $\xi_H$  is related to the semimajor axis  $a$  by  $\xi_H = a/G(\rho)$ , where  $G(\rho) = (1 - \rho^2)^{-0.5} \ln\{\rho^{-1}[1 + (1 - \rho^2)^{0.5}]\}$  and  $\rho$  is the ratio of semiminor axis  $b$  to the semimajor axis  $a$  ( $\rho < 1$ ). The aggregation number  $N_{agg}$  relates to the axis ratio by<sup>28</sup>  $N_{agg} = N_{agg,0}/\rho$ , where  $N_{agg,0}$  is the aggregation number of the minimum spherical micelle. Such calculations show that, at 1.5 M NaCl, the major axis between the entanglements becomes  $19 \pm 4$  nm, with corresponding aggregation number  $450 \pm 100$ , as compared to 60 for the minimum spherical SDS micelle.

The growth of SDS micelles is accompanied by enhanced solubilization of C18 (Figure 2B). In 1.5 M NaCl, the solubility of C18 increases to 16% w/v, which suffices to conduct the micellar copolymerization of C18 and AAc in equimolar mixtures at a total concentration of 1 M. After solubilization of the hydrophobe in aqueous SDS–NaCl solutions, the micellar copolymerization of AAc and C18 was carried out using APS–SMS redox initiator system in the presence of BAAm cross-linker at a cross-linker ratio of 1/100. Hydrogels with a gel fraction of unity could be obtained at a hydrophobe level (C18 mol %) between 20% and 50%. The hydrogels equilibrium swollen in water contained 61–84% water that increased with decreasing C18% or initial monomer concentration (Table S1).

Thermal behavior of water-swollen hydrogels was investigated by DSC as well as by rheometry using oscillatory deformation tests. The gel samples were subjected to heating and cooling cycles between 5 and 80 °C, during which the changes in the heat flux and in the dynamic moduli of gels were monitored as a function of temperature. In Figure 3A, the variations of the elastic modulus  $G'$  and the viscous modulus  $G''$  of a hydrogel sample formed at 35 mol % C18 are shown during the course of the heating and cooling periods. DSC traces of the hydrogels are also shown in the figure by the dashed curves. DSC curves reveal that the swollen hydrogel melt and crystallize with a change in temperature. During cooling of the gel sample from 80 to 5 °C, an exothermic peak appears at 43 °C, corresponding to the crystallization temperature  $T_{cr}$ . During heating back to 80 °C, the swollen gel melts as evidenced from the endothermic peak at 49 °C, corresponding to the melting temperature  $T_m$ . Figure 3A also shows that, at the transition temperatures, both elastic  $G'$  and viscous moduli  $G''$  drastically change due to the formation and dissolution of the crystalline domains in the gel sample. Simultaneously, the loss factor  $\tan \delta (= G''/G')$  changes between below and above 0.1 (not shown in the figure), demonstrating weak-to-strong gel transitions. The change in the moduli of the

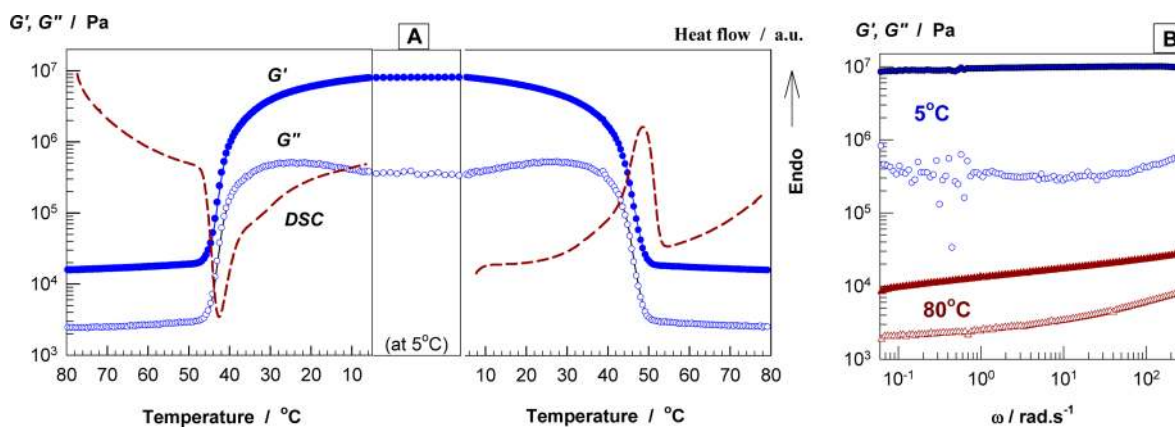


**Figure 3.** (A) Viscoelastic behavior and DSC curve of the hydrogel with 35% C18 during the cooling–heating cycle between 80 and 5 °C.  $C_0 = 1$  M, water content = 63%,  $\omega = 6.28$  rad/s, and  $\gamma_0 = 0.001$ . (B)  $G'$  (filled symbols) and  $G''$  (open symbols) of the hydrogel at 5 and 80 °C shown as a function of the frequency  $\omega$ .  $\gamma_0 = 0.001$ .

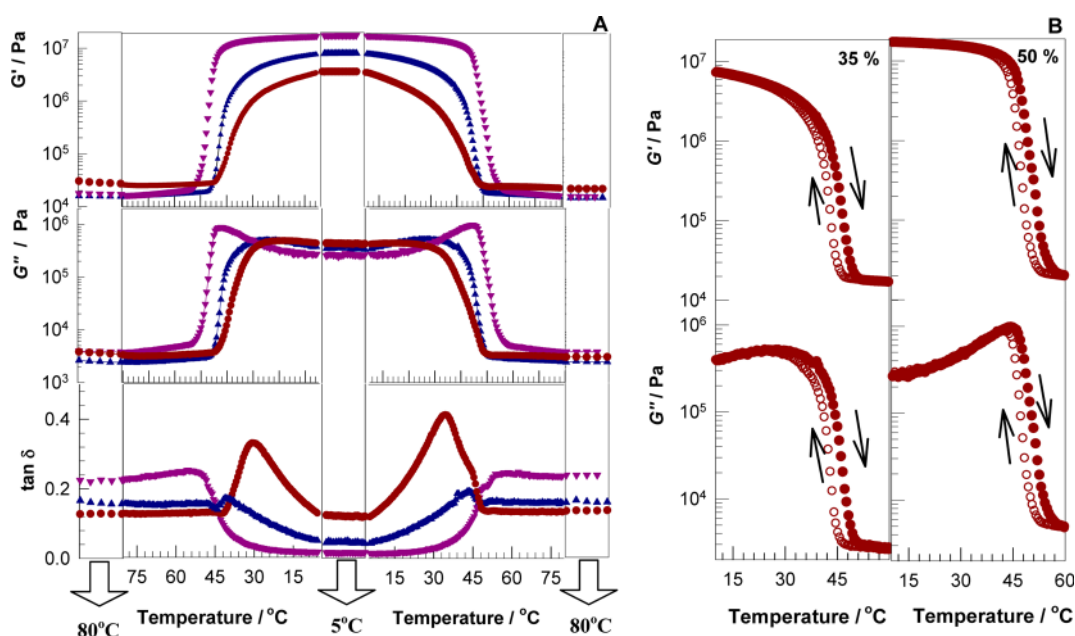


**Figure 4.** (A) Viscoelastic behavior of the hydrogels with various C18 contents during the cooling–heating cycle between 80 and 5 °C.  $C_0 = 1$  M. C18 = 20 (●), 35 (▲), and 50 mol % (▼). (B)  $G'$  and  $G''$  of the hydrogels during the heating–cooling cycle. Arrows show the direction of the temperature change.  $C_0 = 1$  M. C18 mol % indicated.  $\omega = 6.28$  rad/s and  $\gamma_0 = 0.001$ .

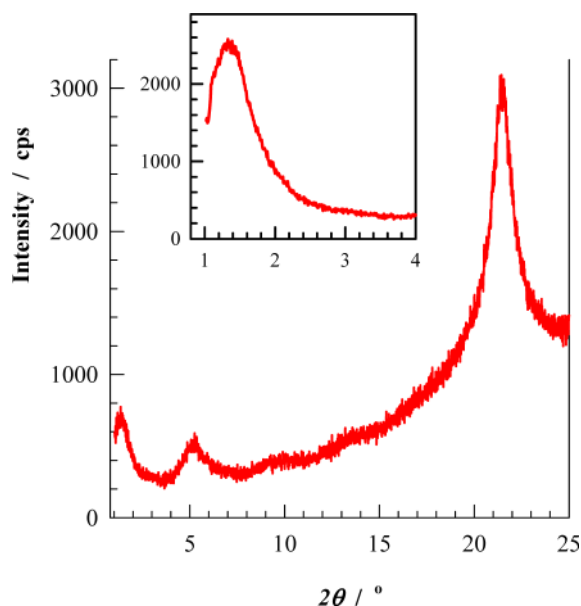
gels depending on the temperature was fully reversible in several cycles (Table S1 and Figure S3).

Figure 3B shows the frequency dependencies of  $G'$  (filled symbols) and  $G''$  (open symbols) for the gels at 80 and 5 °C. At 80 °C, the gel exhibits frequency-dependent dynamic moduli with a loss factor  $\tan \delta$  around 0.2, which is typical for weak gels. Increasing hydrophobe level from 20 to 50% slightly increased  $\tan \delta$  of the hydrogels at 80 °C indicating that the viscous component of the complex modulus increases more than its elastic component (Figure S3). This is attributed to the side chain motions of C18 segments creating energy dissipation. After cooling back to 5 °C, the dynamic moduli become nearly frequency independent and the loss factor decreases to 0.03 corresponding solid-like behavior.  $G''$  values at 5 °C show some scatter due to the sensitivity limit of the rheometer in the determination of the phase angle  $\delta$ .

The extent of the change in the dynamic moduli of gels was strongly dependent on the hydrophobe level. Figure 4A shows

the viscoelastic behavior of the hydrogels formed at various amounts of C18 during the course of the cooling–heating cycle. As the hydrophobe level is increased from 20 to 50%,  $G'$  at 5 °C also increases while the loss factor attains smaller values. The gel with 50% C18 undergoes a reversible 3 orders of magnitude change in the elastic modulus between 80 and 5 °C, i.e., between 17 kPa and 18 MPa (Table S1). Such a large difference in the modulus below and above the transition temperature is the most significant factor to induce the shape memory behavior. The melting  $T_m$  and crystallization temperatures  $T_{cry}$ , determined by DSC measurements, are  $48 \pm 2$  °C and  $43 \pm 2$  °C, respectively, independent of the hydrophobe level of the hydrogels. The hysteresis behavior, that is, the melting occurs at a higher temperature than crystallization was also observable in the viscoelastic behavior of the hydrogels (Figure 4B). During heating from 5 to 80 °C, the drastic changes in the dynamic moduli of gels occur at a higher temperature than during cooling back to 5 °C.

Although both  $T_m$  and  $T_{cry}$  are independent of the amount of C18, the enthalpy change during melting ( $\Delta H_m$ ) per mole of C18 unit in the hydrogel increased with rising level of the hydrophobe. For the hydrogels with 20, 35, and 50 mol % C18,  $\Delta H_m$  was calculated as 28, 31, and 43 kJ/mol, respectively. Assuming that  $\Delta H_m$  is 71.2 kJ for the melting of 1 mol of crystalline C18 units,<sup>31</sup> this indicates an increase in the degree of crystallinity from 40 to 60% as the amount of C18 is increased from 20 to 50 mol %. Figure 5 shows the XRD patterns of the



**Figure 5.** XRD pattern of the hydrogel with 50 mol % C18 in the 1–25°  $2\theta$  range with a scan rate of 1°/min. The inset shows 1–4°  $2\theta$  range with 0.5°/min scan rate.

swollen gel sample with 50% C18. The gel exhibits a crystalline peak at 21.4° corresponding to a Bragg  $d$ -spacing of 0.42 nm. This Bragg  $d$ -spacing is typical for the paraffin-like hexagonal lattices formed by the packing of  $n$ -alkyl chains.<sup>16,32,33</sup> Besides this peak, a second-order diffraction peak at 5.4° and a sharp peak at a very low angle (1.4°) is apparent. The latter corresponding to lattice spacing of 6.3 nm was also observed in C18-containing hydrogels formed in organic media.<sup>16</sup> As discussed before,<sup>16,21</sup> this spacing indicates that C18 side chains form tail-to-tail alignment perpendicularly to the main chains.

In addition to the hydrophobe level, water content of the hydrogels also affected the temperature-dependent changes in their elastic moduli. Figure 6 shows the viscoelastic behavior of the hydrogels with 35% C18 containing 46 and 75% water. At 5 °C, the elastic modulus of the hydrogel increases from 8 to 15 MPa by decreasing its water content from 75 to 46%. Thermoresponsive behavior of the hydrogels was also affected by the presence of SDS (Figure S4), this fact being attributed to the weakening of the hydrophobic interactions due to the surfactant micelles.<sup>13</sup> As mentioned in the Introduction, Osada and co-workers also prepared hydrogels from C18 and AAC monomers by random copolymerization in organic media.<sup>16</sup> To compare the thermal behavior of the present gels with those of Osada, we prepared both types of gels at the same hydrophobe level (35%) and water content (46%). Temperature-dependent variations of the dynamic moduli and the loss factor of the hydrogels are illustrated in Figure 7. In contrast to 120-fold change in  $G'$  of the hydrogels formed by random polymerization, present hydrogels exhibit 1000-fold change in  $G'$  in response to temperature changes. This difference mainly occurs due to the lower modulus and higher loss factor of the present gels in their amorphous states, i.e., at high temperatures. Since hydrophobe level is fixed in both gels, blocky structure of the polymer chains formed by micellar polymerization necessarily reduces the number of blocks per chain. This would decrease the number

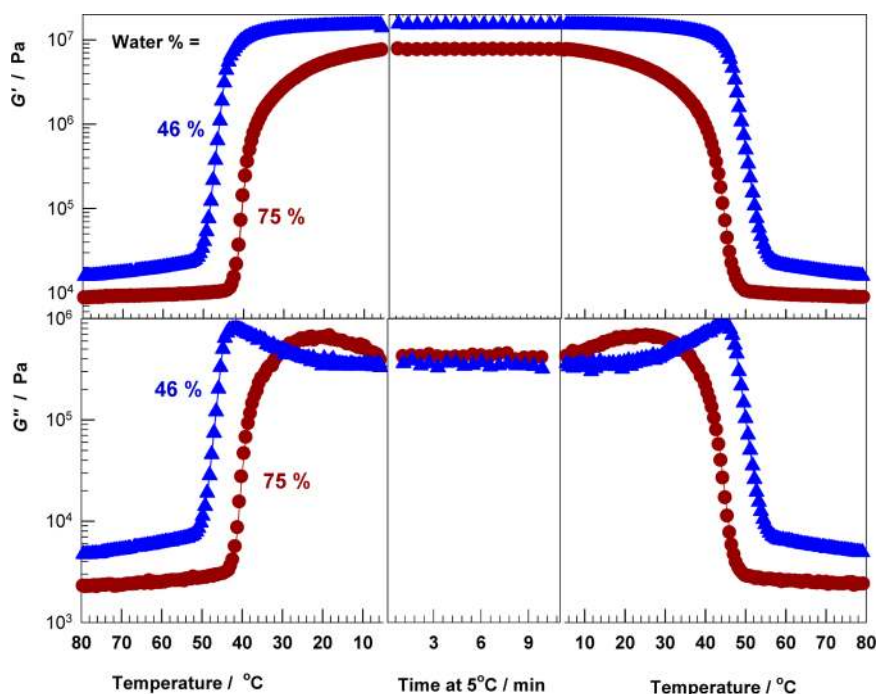


**Figure 6.**  $G'$  and  $G''$  of the hydrogels during the cooling–heating cycle between 80 and 5 °C.  $C_0 = 0.75$  M, C18 = 35 mol %, and  $X = 1/100$ . Water contents are indicated.  $\omega = 6.28$  rad/s and  $\gamma_0 = 0.001$ .

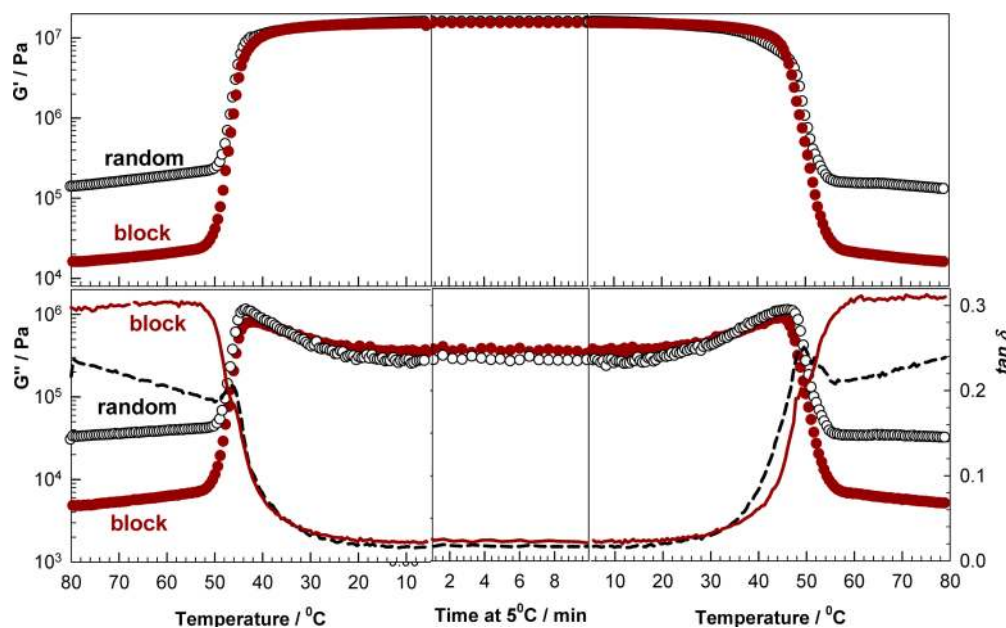


**Figure 7.** Viscoelastic behavior of the hydrogels prepared by random and micellar polymerization during the cooling–heating cycle between 80 and 5 °C. C18 = 35 mol %, water content = 46%,  $\omega = 6.28$  rad/s, and  $\gamma_0 = 0.001$ .

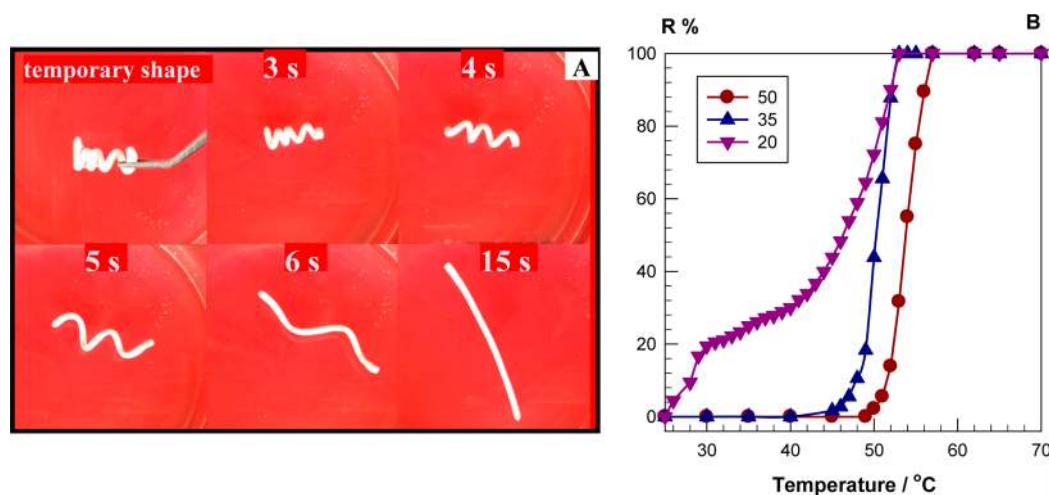


**Figure 8.** (A) Images demonstrating the transition from the temporary shape (spiral) to the permanent shape (rod) for the hydrogel with 50% C18. The recovery takes about 20 s after immersing the gel sample in a water bath at 60 °C. (B) Shape recovery ratio  $R$  of the hydrogels shown as a function of temperature. C18 mol % of the hydrogels indicated.

of hydrophobic associations as compared to the chains containing randomly distributed single hydrophobic units, leading to lower modulus. Indeed, visual observations also showed that, at 80 °C, present gels were too weak as compared to those formed by random copolymerization.

Figure 8A and the movie attached as the Supporting Information demonstrate the shape memory behavior of a hydrogel sample with 50% C18. The permanent shape of the sample is rodlike. After heating to 60 °C, the gel became soft and could easily be deformed to a spiral shape. This temporary shape was fixed by cooling the sample to 24 °C. Immersing the gel sample in a water bath at 60 °C, it returned to its initial shape within 20 s. The covalently cross-linked network structure of the hydrogel determines the permanent (rod) shape while crystalline domains formed by C18 blocks act as switching segments with transition temperature to fix the temporary (spiral) shape. Cylindrical hydrogel samples were also stretched at 60 °C to 6

times their original lengths, and then the temporary shapes were fixed by cooling to room temperature. When immersed in water at 60 °C, the samples recovered their permanent shapes within a few seconds (movie 2, Supporting Information). The principle of thermoresponsive shape memory effect of hydrophobically modified hydrogels is that the covalently cross-linked network structure restores its random coil conformation when the temperature is elevated above the melting temperature of crystalline domains.

To quantify shape memory properties of the hydrogels, the shape recovery ratio  $R$  was recorded at various temperatures. The results are shown in Figure 8B where  $R$  of the hydrogels is plotted against the temperature. All hydrogel samples exhibited shape-recovery ratios of 100% at or above 57 °C. For the hydrogels with 35 and 50% C18, the recovery ratio  $R$  is equal to zero below 45 and 50 °C, respectively, indicating that the temporary shape remains unchanged; that is, the shape fixing efficiency is 100%.

This reveals the ability of these gel samples to hold the temporary shape up to temperatures close to the transition temperature. In contrast, for the hydrogel with 20% C18, the shape recovery ratio gradually increases with increasing temperature, indicating that the crystalline domains in this sample cannot support the residual stress in the network chains. This is consistent with the low degree of crystallinity of this hydrogel (40%) and its viscoelastic nature with  $\tan \delta = 0.12$  (Figure 4A and Table S1). Thus, the shape fixing efficiency of the hydrogels can be controlled by the degree of crystallinity, which in turn depends on the hydrophobe content of the hydrophilic network chains.

## CONCLUSIONS

The synthesis of shape memory hydrogels using micellar polymerization was reported for the first time. The copolymerization of AAC and C18 was performed in an aqueous solution of wormlike SDS micelles. Swollen hydrogels containing 61–84% water melt and crystallize with a change in temperature. Independent of the hydrophobe level between 20 and 50 mol %, the melting and crystallization temperatures of the hydrogels are  $48 \pm 2$  °C and  $43 \pm 2$  °C, respectively. The hydrogels exhibit 3 orders of magnitude change in the elastic modulus when the temperature changes between below and above the melting temperature of the crystalline domains. The blocky structure of the polymers formed by micellar polymerization is responsible for the drastic change in their mechanical properties and significant shape memory effect. The unique shape memory properties of the hydrogels, the simplicity of their preparation, their availability from a wide variety of monomer systems, and the adjustability of the hydrophobic block length by the size of surfactant micelles hold promise well for future applications.

## ASSOCIATED CONTENT

### Supporting Information

Table S1, properties of shape memory hydrogels; Figure S1, solubility of C18 in aqueous SDS–NaCl solutions; Figure S2, DSC curves of the hydrogels formed by random polymerization; Figures S3 and S4, effects of temperature and SDS on the viscoelastic behavior of shape memory hydrogels; and the movies demonstrating the shape memory behavior of the hydrogels. This material is available free of charge via the Internet at <http://pubs.acs.org>.

## AUTHOR INFORMATION

### Corresponding Author

\*E-mail [okayo@itu.edu.tr](mailto:okayo@itu.edu.tr).

### Notes

The authors declare no competing financial interest.

## ACKNOWLEDGMENTS

Work was supported by the Scientific and Technical Research Council of Turkey (TUBITAK) and International Bureau of the Federal Ministry of Education and Research of Germany (BMBF), TBAG-109T646. O.O. thanks Turkish Academy of Sciences (TUBA) for the partial support.

## REFERENCES

- (1) Candau, F.; Selb, J. *Adv. Colloid Interface Sci.* **1999**, *79*, 149.
- (2) Volpert, E.; Selb, J.; Candau, F. *Polymer* **1998**, *39*, 1025.
- (3) Hill, A.; Candau, F.; Selb, J. *Macromolecules* **1993**, *26*, 4521.
- (4) Regalado, E. J.; Selb, J.; Candau, F. *Macromolecules* **1999**, *32*, 8580.
- (5) Candau, F.; Regalado, E. J.; Selb, J. *Macromolecules* **1998**, *31*, 5550.

- (6) Kujawa, P.; Audibert-Hayet, A.; Selb, J.; Candau, F. *J. Polym. Sci., Part B: Polym. Phys.* **2004**, *42*, 1640.
- (7) Kujawa, P.; Audibert-Hayet, A.; Selb, J.; Candau, F. *Macromolecules* **2006**, *39*, 384.
- (8) Gao, B.; Guo, H.; Wang, J.; Zhang, Y. *Macromolecules* **2008**, *41*, 2890.
- (9) Chern, C. S.; Chen, T. J. *Colloids Surf., A* **1998**, *138*, 65.
- (10) Leyrer, R. J.; Machtle, W. *Macromol. Chem. Phys.* **2000**, *201*, 1235.
- (11) Lau, W. *Macromol. Symp.* **2002**, *182*, 283.
- (12) Tuncaboylu, D. C.; Sari, M.; Oppermann, W.; Okay, O. *Macromolecules* **2011**, *44*, 4997.
- (13) Tuncaboylu, D. C.; Sahin, M.; Argun, A.; Oppermann, W.; Okay, O. *Macromolecules* **2012**, *45*, 1991.
- (14) Tuncaboylu, D. C.; Argun, A.; Sahin, M.; Sari, M.; Okay, O. *Polymer* **2012**, *53*, 5513.
- (15) Akay, G.; Hassan-Raeisi, A.; Tuncaboylu, D. C.; Orakdogan, N.; Abdurrahmanoglu, S.; Oppermann, W.; Okay, O. *Soft Matter* **2013**, *9*, 2254.
- (16) Matsuda, A.; Sato, J.; Yasunaga, H.; Osada, Y. *Macromolecules* **1994**, *27*, 7695.
- (17) Osada, Y.; Matsuda, A. *Nature* **1995**, *376*, 219.
- (18) Tanaka, Y.; Kagami, Y.; Matsuda, A.; Osada, Y. *Macromolecules* **1995**, *28*, 2574.
- (19) Uchida, M.; Kurosawa, M.; Osada, Y. *Macromolecules* **1995**, *28*, 4583.
- (20) Miyazaki, T.; Kaneko, T.; Gong, J. P.; Osada, Y. *Macromolecules* **2001**, *34*, 6024.
- (21) Miyazaki, T.; Yamaoka, K.; Gong, J. P.; Osada, Y. *Macromol. Rapid Commun.* **2002**, *23*, 447.
- (22) Lin, X. K.; Chen, L.; Zhao, Y. P.; Dong, Z. Z. *J. Mater. Sci.* **2010**, *45*, 2703.
- (23) Inomata, K.; Terahama, T.; Sekoguchi, R.; Ito, T.; Sugimoto, H.; Nakanishi, E. *Polymer* **2012**, *53*, 3281.
- (24) Hao, J.; Weiss, R. A. *ACS Macro Lett.* **2013**, *2*, 89.
- (25) ISO 7875-1, 1996. Water quality. Determination of surfactants. Part 1: Determination of anionic surfactants by measurement of the methylene blue index (MBAS). ISO/TC 147.
- (26) Liu, G.; Ding, X.; Cao, Y.; Zheng, Z.; Peng, Y. *Macromolecules* **2004**, *37*, 2228.
- (27) (a) Rehage, H.; Hoffman, H. *Mol. Phys.* **1991**, *74*, 933. (b) Missel, P. J.; Mazer, N. A.; Benedek, G. B.; Young, C. Y. *J. Phys. Chem.* **1980**, *84*, 1044. (c) Magid, L. J. *J. Phys. Chem. B* **1998**, *102*, 4064. (d) Hassan, P. A.; Raghavan, S. R.; Kaler, E. W. *Langmuir* **2002**, *18*, 2543. (e) Sutherland, E.; Mercer, S. M.; Everist, M.; Leaist, D. *J. Chem. Eng. Data* **2009**, *54*, 272.
- (28) Mazer, N. A.; Benedek, G. B.; Carey, M. C. *J. Phys. Chem.* **1976**, *80*, 1075.
- (29) Young, C. Y.; Missel, P. J.; Mazer, N. A.; Benedek, G. B.; Carey, M. C. *J. Phys. Chem.* **1978**, *82*, 1375.
- (30) Pecora, R. *Dynamic Light Scattering: Application of Photon Correlation Spectroscopy*; Plenum Press: New York, 1985.
- (31) (a) Mogri, Z.; Paul, D. R. *Polymer* **2001**, *42*, 2531. (b) Bisht, H. S.; Pande, P. P.; Chatterjee, A. K. *Eur. Polym. J.* **2002**, *38*, 2355.
- (32) Plate, N. A.; Shibaeva, V. P. *J. Polym. Sci., Macromol. Rev.* **1974**, *8*, 117.
- (33) Livshin, S.; Silverstein, M. S. *Macromolecules* **2008**, *41*, 3930.